

What Hard Tokens Reveal: Exploiting Low-confidence Tokens for Membership Inference Attacks against Large Language Models

Md Tasnim Jawad¹, Mingyan Xiao², Yanzhao Wu¹

¹Florida International University, Miami, Florida, USA

²California State Polytechnic University, Pomona, Pomona, California, USA

mjawa009@fiu.edu, mxiao@cpp.edu, yawu@fiu.edu

Abstract

With the widespread adoption of Large Language Models (LLMs) and increasingly stringent privacy regulations, protecting data privacy in LLMs has become essential, especially for privacy-sensitive applications. Membership Inference Attacks (MIAs) attempt to determine whether a specific data sample was included in the model training/fine-tuning dataset, posing serious privacy risks. However, most existing MIA techniques against LLMs rely on sequence-level aggregated prediction statistics, which fail to distinguish prediction improvements caused by generalization from those caused by memorization, leading to low attack effectiveness. To address this limitation, we propose a novel membership inference approach that captures the token-level probabilities for low-confidence (hard) tokens, where membership signals are more pronounced. By comparing token-level probability improvements at hard tokens between a fine-tuned target model and a pre-trained reference model, HT-MIA isolates strong and robust membership signals that are obscured by prior MIA approaches. Extensive experiments on both domain-specific medical datasets and general-purpose benchmarks demonstrate that HT-MIA consistently outperforms seven state-of-the-art MIA baselines. We further investigate differentially private training as an effective defense mechanism against MIAs in LLMs. Overall, our HT-MIA framework establishes hard-token based analysis as a state-of-the-art foundation for advancing membership inference attacks and defenses for LLMs.

1 Introduction

In recent years, Large Language Models (LLMs) have become foundational tools to both industry and research. These models are frequently fine-tuned for various downstream tasks, including clinical decision support (Wu et al., 2023; Wang et al., 2023; Luo et al., 2022; Singhal et al., 2023;

Paiola et al., 2024), scientific research (Beltagy et al., 2019; Taylor et al., 2022), legal document analysis (Chalkidis et al., 2020; Niklaus et al., 2024; Tewari, 2024), education and intelligent tutoring (Ross et al., 2025; Scarlatos et al., 2025; Hosen, 2025), and cybersecurity (Jin et al., 2024; Sanchez et al., 2025). Many of these settings involve sensitive or regulated data, making privacy protection a central concern in LLMs. A key privacy threat in this context is Membership Inference Attacks (MIAs), which aim to determine whether a specific data sample was included in a model’s training or fine-tuning dataset (Shokri et al., 2017; Hu et al., 2022; Galileo, 2025). A successful MIA can reveal sensitive information about individuals, institutions, or proprietary datasets, raising serious concerns about regulatory compliance and data privacy. Prior studies have demonstrated the privacy risks posed by MIAs across multiple domains (Zhong et al., 2024; Zhang et al., 2023, 2022). Despite these risks, executing effective MIAs against modern LLMs remains challenging. Strong generalization during LLM pre-training and fine-tuning often causes member and non-member samples to exhibit highly similar aggregated prediction behaviors, weakening traditional membership signals (Duan et al., 2024b). As a result, most existing MIA studies that rely on sequence-level aggregated prediction statistics (Meeus et al., 2024) frequently report low attack success against well-generalized LLMs (fuzzy labs, 2025).

To address this issue, we propose a novel approach that focuses on low-confidence (Hard) Tokens for conducting Membership Inference Attacks (HT-MIA). By comparing token-level probability improvements between a target model and a reference model, our approach isolates strong and robust membership signals that are obscured by prior MIA methods. We benchmark HT-MIA against seven state-of-the-art MIA methods and demonstrate consistent performance improvements

across four datasets spanning both medical and general domains. In addition, we conduct an ablation study to validate the effectiveness of our design choices, analyze why traditional approaches tend to fail, and investigate potential defense strategies against membership inference risks for LLMs.

2 Problem Statement

In this work, we primarily focus on MIAs in the LLM fine-tuning settings. Unlike large-scale LLM pre-training, where datasets are massive, heterogeneous, and often opaque (Businessinsider, 2025; Achiam et al., 2023), fine-tuning typically adapts a pre-trained LLM to a smaller, task-specific dataset that may contain sensitive or regulated information (e.g., medical data). This setting introduces a more realistic and practically relevant threat model for evaluating MIAs, as membership labels can be clearly defined based on the separation between member and non-member samples in the fine-tuning data split. Moreover, fine-tuning is also the dominant paradigm for deploying LLMs in real-world applications, making it a critical context in which to assess and understand membership inference risks. We note that the proposed HT-MIA framework is not inherently restricted to fine-tuning and is also applicable to pre-training settings.

Target Model: The attack target models are obtained by fine-tuning a pre-trained LLM on domain-specific datasets (Jin et al., 2023; Jeong, 2024; Anisuzzaman et al., 2025). These LLMs predict the next token in a sequence conditioned on the preceding context. Given a sample sequence of tokens $x = [x_1, x_2, \dots, x_n]$, the target model assigns a probability distribution over the sequence by factorizing it as

$$P_\theta(x) = \prod_{i=1}^n P_\theta(x_i | x_{<i}), \quad (1)$$

where $P_\theta(x_i | x_{<i})$ denotes the prediction probability assigned to token x_i given the prefix $x_{<i}$ (Song et al., 2024) and θ represents the model parameters. Fine-tuning is performed by minimizing the negative log-likelihood loss:

$$\mathcal{L}(\theta) = - \sum_{i=1}^n \log P_\theta(x_i | x_{<i}). \quad (2)$$

The ground-truth tokens are provided at each step (Malladi et al., 2023; Chang et al., 2024). We regard the corresponding pre-trained LLM, prior to fine-tuning, as the reference (Ref.) model \mathcal{B} .

Threat Model: We consider an adversary who aims to infer whether a sample sequence x was included in the training split (D_{mem}) of the fine-tuning dataset D for the target model \mathcal{F} . The dataset D is partitioned, such that $D = D_{\text{mem}} \cup D_{\text{non-mem}}$ and $D_{\text{mem}} \cap D_{\text{non-mem}} = \emptyset$, where D_{mem} and $D_{\text{non-mem}}$ represent the member (training) and non-member partitions, respectively.

The adversaries are assumed to have query access to \mathcal{F} , allowing them to obtain model outputs such as probabilities, logits, or generated responses for arbitrary inputs. To conduct membership inference attacks, the adversary extracts a *membership signal* $S(x; \mathcal{F})$ from model outputs. This signal can take different forms, such as the confidence assigned to x , the loss value, or a calibrated score derived from comparing multiple models (He et al., 2024). The adversary applies a decision rule as

$$g(x; \mathcal{F}) = \begin{cases} \text{member}, & \text{if } S(x; \mathcal{F}) \geq \tau, \\ \text{non-member}, & \text{otherwise.} \end{cases} \quad (3)$$

Here, τ is a threshold chosen by the adversary. A prediction of *member* indicates that x is inferred to belong to the training set D_{mem} ($x \in D_{\text{mem}}$), while *non-member* indicates the opposite (Mireshghal-lah et al., 2022). Unlike the free-running mode of generation, an LLM can expose MIA signals under *teacher-forced next-token prediction* (Chang et al., 2024). In this setting, the model receives the ground-truth sequence prefix $r_{<i}$ as input and is supervised to predict the next ground-truth token r_i . This setup allows direct measurement of token-level signals over the sample sequence x (Bachmann and Nagarajan, 2024).

3 HT-MIA Overview

We present the overall workflow of our proposed HT-MIA framework in Figure 1. Our method, builds on the idea of extracting token-level probabilities for low-confidence (hard) tokens within a given sequence sample. Specifically, we perform a *teacher-forced forward pass* for both the fine-tuned target model \mathcal{F} and the reference model \mathcal{B} . The full algorithm is presented in Algorithm 1.

The key intuition is that non-member samples behave similarly for both target (\mathcal{F}) and reference (\mathcal{B}) models, while the fine-tuned model \mathcal{F} assigns systematically higher probabilities than the reference model \mathcal{B} to member samples, especially at hard-to-predict tokens with low confidence. Con-

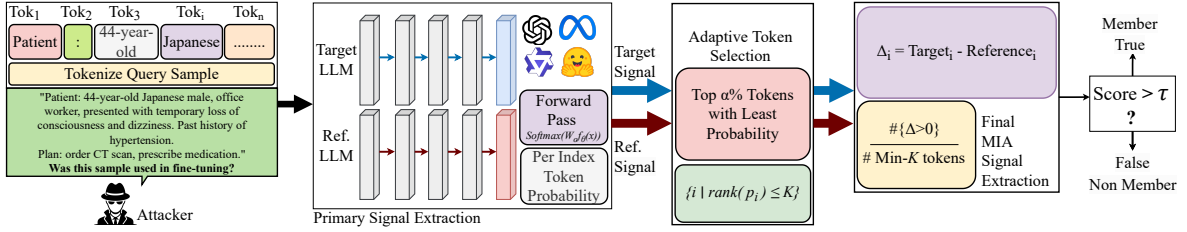


Figure 1: Overall Workflow of HT-MIA.

Algorithm 1 HT-MIA for a Single Text

```

Input: Text  $x$ ; fine-tuned model  $\mathcal{F}$ ; reference model  $\mathcal{B}$ ; shared tokenizer  $\tau$ ; integers  $\text{min\_k}$ ,  $\text{max\_k}$ ; limit  $\text{max\_length}$ ; proportion  $\alpha \in (0, 1]$ .
Output: HT-MIA Score  $s \in [0, 1]$ .
1:  $t \leftarrow \tau.\text{ENCODE}(x, \text{max\_length})$ 
2: if  $K = 0$  then return 0.5
3:  $\ell^{\mathcal{F}} \leftarrow \mathcal{F}(t).\text{LOGITS}$ ;  $\ell^{\mathcal{B}} \leftarrow \mathcal{B}(t).\text{LOGITS}$ 
4:  $p^{\mathcal{F}} \leftarrow \text{SOFTMAX}(\ell^{\mathcal{F}})$ ;  $p^{\mathcal{B}} \leftarrow \text{SOFTMAX}(\ell^{\mathcal{B}})$ 
5: for  $i = 1$  to  $|t| - 1$  do
6:    $y_i \leftarrow t_{i+1}$ 
7:    $q_i^{\mathcal{F}} \leftarrow p^{\mathcal{F}}[i, y_i]$ ;  $q_i^{\mathcal{B}} \leftarrow p^{\mathcal{B}}[i, y_i]$ 
8: end for                                 $\triangleright$  Per-token probability extraction
9:  $L \leftarrow |t| - 1$ 
10:  $K \leftarrow \min(\text{max\_k}, \max(\text{min\_k}, \lfloor \alpha L \rfloor))$ 
11:  $K \leftarrow \min(K, L)$ 
12: if  $K = 0$  then return 0.5  $\triangleright$  Adaptive token selection
13:  $I_{\text{min}} \leftarrow \text{ARGSORTASCENDING}(q^{\mathcal{F}})[1:K]$ 
14:  $\Delta \leftarrow \{q_i^{\mathcal{F}} - q_i^{\mathcal{B}} \mid i \in I_{\text{min}}\}$ 
15:  $s \leftarrow \frac{1}{K} \sum_{i \in I_{\text{min}}} \mathbf{1}\{\Delta_i > 0\}$   $\triangleright$  Membership inference score
16: return  $s$ 

```

cretely, for a given text prompt x :

- If x is not a member of the training/fine-tuning dataset (*non-member*), \mathcal{F} and \mathcal{B} assign similar probabilities.
- If x is a *member* of the training/fine-tuning dataset, \mathcal{F} assigns *higher* probabilities than \mathcal{B} , particularly at inherently hard-to-predict tokens.

Empirically, we observe that tokens with the lowest predicted probability under \mathcal{F} provide the most informative membership signals. Improvements at these positions are more indicative of memorization effects introduced during LLM fine-tuning, rather than generalization. In contrast, differences at high-confidence (easy-to-predict) tokens are typically small and carry limited interpretive value for membership inference.

3.1 Attack Method

Given a text sample x , we perform the following steps:

Step 1: Token probability extraction.

Given a text sample x , the text is first tokenized into a sequence $t_{1:L}$ with corresponding next tokens

$y_{1:L}$. Token-level probabilities are then extracted from both the fine-tuned model \mathcal{F} and reference model \mathcal{B} through teacher-forced forward passes. For each position $i = 1, \dots, L$, the following probabilities are obtained:

$$p_{\mathcal{F},i} = P_{\mathcal{F}}(y_i \mid t_{\leq i}),$$

$$p_{\mathcal{B},i} = P_{\mathcal{B}}(y_i \mid t_{\leq i}).$$

Step 2: Adaptive token selection.

The algorithm identifies the tokens where \mathcal{F} has the lowest confidence by sorting $\{p_{\mathcal{F},i}\}_{i=1}^L$ in ascending order. Let I_{min} denote the indices of the K smallest values, where

$$K = \min(\text{max_k}, \max(\text{min_k}, \lfloor \alpha L \rfloor)), \quad (4)$$

with $\alpha \in (0, 1]$ being a proportion parameter, and min_k , max_k being user-specified bounds. This adaptive selection ensures the method scales appropriately with sequence length while maintaining robustness across both short and long text inputs.

Step 3: Probability improvement computation.

For each selected token index $i \in I_{\text{min}}$, the probability difference is computed as:

$$\Delta_i = p_{\mathcal{F},i} - p_{\mathcal{B},i}. \quad (5)$$

This difference captures the improvement in probability assigned by the fine-tuned target model relative to the reference model.

Step 4: Membership score aggregation.

The **HT-MIA** score is computed by aggregating these per-token comparisons, measuring the fraction of selected tokens where \mathcal{F} outperforms \mathcal{B} :

$$S(x; \mathcal{F}, \mathcal{B}) = \frac{1}{K} \sum_{i \in I_{\text{min}}} \mathbf{1}\{\Delta_i > 0\} \in [0, 1]. \quad (6)$$

A higher score indicates that the fine-tuned model assigns consistently higher probabilities than the reference model at difficult positions, providing evidence of membership. The final decision rule is given by:

$$g(x; \mathcal{F}) = \text{member} \quad \text{iff} \quad S(x; \mathcal{F}, \mathcal{B}) \geq \tau, \quad (7)$$

where τ is a threshold chosen based on the desired false-positive rate. We provide further analysis in Appendix A.

3.2 Defense Method

Considering the practical risks of membership inference attacks, it is essential to explore techniques that limit privacy leakage on training/fine-tuning data. Hence, we also investigate an effective defense against MIA within the HT-MIA framework based on Differentially Private Stochastic Gradient Descent (DP-SGD). DP-SGD is a popular training algorithm that provides formal privacy guarantees by limiting the influence of individual training examples on model parameters (Abadi et al., 2016). For each training sample x_i in a batch, DP-SGD first computes the per-example gradient:

$$\mathbf{g}_t(x_i) = \nabla_{\theta_t} \mathcal{L}(\theta_t, x_i).$$

These gradients are then clipped to bound their ℓ_2 norm by a threshold C :

$$\bar{\mathbf{g}}_t(x_i) \leftarrow \mathbf{g}_t(x_i) / \max \left(1, \frac{\|\mathbf{g}_t(x_i)\|_2}{C} \right).$$

Finally, calibrated Gaussian noise is added to the aggregated clipped gradients:

$$\tilde{\mathbf{g}}_t \leftarrow \frac{1}{K} \left(\sum_i \bar{\mathbf{g}}_t(x_i) + \mathcal{N}(0, \sigma^2 C^2 \mathbf{I}) \right).$$

The key hyperparameters (noise multiplier σ , clipping norm C , and batch size K) are carefully tuned to balance model utility against privacy protection (Abadi et al., 2016).

4 Experimental Analysis

Target Model Configurations: To evaluate our HT-MIA framework, we experiment with 3 instances of the target model \mathcal{F} , spanning different sizes and architectures. Specifically, we fine-tuned GPT-2 (Radford et al., 2019), Qwen-3-0.6B (Yang et al., 2025), and LLaMA-3.2-1B (Dubey et al., 2024) as the target models. For our main experiments, we use the corresponding pre-trained base versions of these models as the reference model. In addition, we evaluate a more practical scenario where the exact pre-trained version of the target model is not available. In this scenario, we compared the target model with other reference models, including Qwen2.5-0.5B (Yang et al., 2025) and DistilGPT-2 (Sanh et al., 2019).

Datasets: To construct membership and non-membership samples, we utilized four publicly available datasets. For the medical domain, we employ the Augmented Clinical Notes dataset (Bonnet et al., 2023) (referred to as Clinicalnotes) and the Asclepius Synthetic Clinical Notes dataset (Kweon et al., 2023) (referred to as Asclepius). For broader

coverage, we fine-tuned LLMs on the IMDB Large Movie Review dataset (Maas et al., 2011) and the Wikipedia text corpus (Wikipedia, 2022). This combination enables a comprehensive evaluation of membership inference risks across domain-specific and general-purpose settings. For all datasets, we adopt a 50:50 split between training and validation data, resulting in equally sized member D_{mem} and non-member $D_{\text{non-mem}}$ sets.

Baselines: We compare HT-MIA against seven representative MIA baselines spanning major categories, including loss-based (**Loss** (Yeom et al., 2018)), perturbation-based (**Lowercase** (Carlini et al., 2021), **PAC** (Ye et al., 2024), **SPV-MIA** (Fu et al., 2023)), token-level (**Min-K++** (Zhang et al., 2024a)), reference-based (**Ratio** (Carlini et al., 2021)), and compression-based (**Zlib** (Carlini et al., 2021)) approaches. The majority of these methods utilize the full input sequence, diluting the MIA signal. Unlike Min-K++, HT-MIA leverages a reference model to guide the exploitation of informative low-confidence tokens. Compared to Ratio’s full-sequence likelihood ratios, HT-MIA focuses exclusively on low-confidence tokens where membership information is most concentrated. Detailed descriptions for all baseline methods are provided in Appendix B.

We also provide details regarding the evaluation metrics in Appendix C.

4.1 Overall Performance

In this section, we highlight the collective findings of our main experiments. Overall, HT-MIA outperforms all baselines across three out of four datasets. On **Asclepius**, it achieves the highest AUC on all three models: 73.48% (LLaMA-3.2-1B), 73.12% (Qwen-3-0.6B), and 56.79% (GPT-2), surpassing Ratio and Min-K++ by 5-6% on the first two models. For TPR@FPR=0.1, HT-MIA substantially improves recall on LLaMA-3.2-1B (37.07% vs. 23.30%) and outperforms all methods at TPR@FPR=0.01 across all models. On **Clinicalnotes**, HT-MIA achieves the highest AUC: 86.59% (LLaMA-3.2-1B), 88.43% (Qwen-3-0.6B), and 69.78% (GPT-2). It shows consistent gains at TPR@FPR=0.01, with improvements of up to 10% over the best baselines. On **Wikipedia**, HT-MIA establishes clear superiority with 86.2% (LLaMA-3.2-1B) and 91.0% (Qwen-3-0.6B), outperforming Ratio by 4.7% and 7.3% respectively. On **IMDB**, HT-MIA remains highly competitive with 92.3% (LLaMA-3.2-1B) and 94.7% (Qwen-3-0.6B), trail-

Method	LLaMA-3.2-1B	Qwen-3-0.6B	GPT-2
Loss	0.6332	0.6322	0.5347
Lowercase	0.6137	0.6166	0.5431
Min-K++	0.6084	0.6103	0.5324
PAC	0.6156	0.6225	0.5300
Ratio	0.6749	0.6819	0.5332
Zlib	0.6380	0.6365	0.5366
SPV-MIA	0.6399	0.6491	0.5445
HT-MIA	0.7348	0.7312	0.5679

Method	LLaMA-3.2-1B	Qwen-3-0.6B	GPT-2
Loss	0.1970	0.1888	0.1202
Lowercase	0.1796	0.1799	0.1254
Min-K++	0.1623	0.1545	0.1151
PAC	0.1734	0.1775	0.1157
Ratio	0.2330	0.2205	0.1170
Zlib	0.1977	0.1905	0.1207
SPV-MIA	0.2170	0.2720	0.1310
HT-MIA	0.3707	0.3129	0.1109

Method	LLaMA-3.2-1B	Qwen-3-0.6B	GPT-2
Loss	0.0228	0.0220	0.0131
Lowercase	0.0247	0.0236	0.0144
Min-K++	0.0182	0.0149	0.0127
PAC	0.0189	0.0194	0.0116
Ratio	0.0271	0.0250	0.0120
Zlib	0.0239	0.0225	0.0131
SPV-MIA	0.0210	0.0410	0.0090
HT-MIA	0.0817	0.0477	0.0181

(a) AUC

(b) TPR@FPR=0.1

(c) TPR@FPR=0.01

Table 1: Comparison of AUC, TPR@FPR=0.1, and TPR@FPR=0.01 across LLaMA-3.2-1B, Qwen-3-0.6B, and GPT-2 fine-tuned on the Asclepius dataset.

Method	LLaMA-3.2-1B	Qwen-3-0.6B	GPT-2
Loss	0.8212	0.8100	0.6238
Lowercase	0.7511	0.7332	0.5651
Min-K++	0.8000	0.7649	0.6336
PAC	0.7982	0.8001	0.5886
Ratio	0.8642	0.8681	0.6440
Zlib	0.7998	0.7838	0.5954
SPV-MIA	0.5266	0.8359	0.6233
HT-MIA	0.8659	0.8843	0.6978

(a) AUC

(b) TPR@FPR=0.1

(c) TPR@FPR=0.01

Table 2: Comparison of AUC, TPR@FPR=0.1, and TPR@FPR=0.01 across LLaMA-3.2-1B, Qwen-3-0.6B, and GPT-2 fine-tuned on the Clinicalnotes dataset.

ing only Ratio while surpassing all other methods by a clear margin.

We discuss these results in detail in Section 4.2 and Section 4.3.

4.2 Medical Dataset

Asclepius dataset: Table 1 reports the performance of HT-MIA against baseline attack methods on LLaMA-3.2-1B, Qwen-3-0.6B, and GPT-2 fine-tuned on Asclepius dataset. Highlighted in Table 1a, HT-MIA achieves the highest AUC across all three target models. On LLaMA-3.2-1B and Qwen-3-0.6B, our method attains 73.48% and 73.12%, surpassing the strongest baseline (Ratio) by 5.99% and 4.93%. For GPT-2, HT-MIA achieves 56.79%, outperforming all baselines by over 2%. While some baselines show competitive performance on specific models, none achieve the consistency of our approach across architectures, demonstrating that our probability improvement metric effectively captures membership signals that single-model and perturbation-based methods fail to isolate.

At relaxed (FPR=0.1, Table 1b) and strict (FPR=0.01, Table 1c) thresholds, HT-MIA consistently outperforms most baselines. At FPR=0.1, our method achieves 37.07% and 31.29% on LLaMA-3.2-1B and Qwen-3-0.6B respectively, improving over the next-best methods by 59.1% and 15.0%. At the stricter FPR=0.01, HT-MIA reaches 8.17%, 4.77%, and 1.81% on the three models,

achieving nearly 4× the TPR of Min-K++ on LLaMA-3.2-1B and 16.3% improvement on Qwen-3-0.6B.

Several key patterns emerge from our analysis. *First*, the performance gap between HT-MIA and baselines widens as the false positive constraint becomes stricter, indicating more confident and well-separated scores. *Second*, larger models exhibit stronger membership signals than GPT-2, likely due to greater memorization capacity. *Third*, while Ratio and Min-K++ consistently rank among top baselines, neither matches our method’s ability to isolate membership-specific improvements through adaptive token selection and cross-model comparison.

Clinicalnotes dataset: Table 2 presents the corresponding results from baseline attack methods on LLaMA-3.2-1B, Qwen-3-0.6B, and GPT-2 fine-tuned on Clinicalnotes dataset. As shown in Table 2a, HT-MIA achieves the highest AUC across all three target models. On GPT-2, it reaches 69.78%, exceeding the next-best baseline (Ratio at 64.40%) by 5.38%. On LLaMA-3.2-1B and Qwen-3-0.6B, it attains 86.59% and 88.43%, surpassing the strongest baseline (Ratio) by 0.17% and 1.62%, respectively. The narrower margins on the larger models compared to GPT-2 suggest that the Clinicalnotes dataset produces stronger membership signals overall, making the detection task easier across most methods. Nevertheless, HT-MIA main-

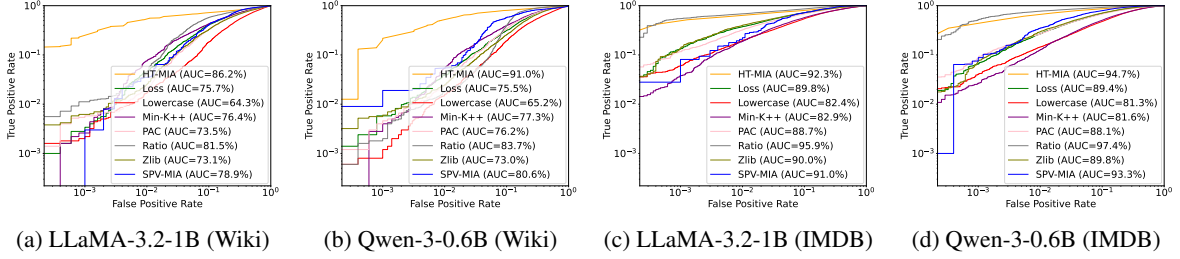


Figure 2: Comparison of multiple MIA methods on target models fine-tuned with Wikipedia and IMDB datasets.

tains its advantage, demonstrating that even when baselines perform relatively well, our probability improvement metric continues to extract additional discriminative information. The consistently high AUC values on LLaMA-3.2-1B and Qwen-3-0.6B show that fine-tuning on medical text introduces greater distributional shifts than Asclepius.

At both FPR thresholds (Tables 2b and 2c), HT-MIA demonstrates strong performance across all models. At FPR=0.1, our method leads on Qwen-3-0.6B (68.61%) and GPT-2 (32.23%) with relative improvements of 6.7% and 55.3% over the best baselines, while Ratio narrowly exceeds HT-MIA by 0.13% on LLaMA-3.2-1B (70.70% vs. 70.57%). At the stricter FPR=0.01, HT-MIA attains the highest TPR across all models: 42.53%, 38.39%, and 5.24%. While Ratio emerges as a strong competitor on larger models with strong membership signals, it falls short of HT-MIA, particularly at lower FPRs.

4.3 General Dataset

Figure 2 presents ROC curves comparing HT-MIA against baseline MIA methods on LLaMA-3.2-1B and Qwen-3-0.6B fine-tuned on the Wikipedia and IMDB datasets.

Wikipedia dataset: On the Wikipedia dataset, HT-MIA achieves the highest AUC across both models: 86.2% on LLaMA-3.2-1B (Figure 2a) and 91.0% on Qwen-3-0.6B (Figure 2b), outperforming the strongest baseline (Ratio) by 4.7% and 7.3% respectively. The next-best methods trail by 6.5–9.8% on LLaMA-3.2-1B and over 10% on Qwen-3-0.6B, with traditional metrics like Loss and Zlib showing even weaker performance. The consistently larger margins on Qwen-3-0.6B suggest that our probability improvement metric is particularly effective at exploiting memorization patterns when fine-tuned on encyclopedic text.

The ROC curves reveal that HT-MIA’s performance advantage becomes more pronounced in the low false positive rate region ($FPR < 0.01$), critical for practical deployment. On both mod-

els, our method maintains substantially higher TPR than all baselines when FPR is constrained below 1%. At $FPR \approx 0.001$, HT-MIA achieves approximately 5–10× higher TPR on LLaMA-3.2-1B and 10–15× on Qwen-3-0.6B compared to the second-best methods. This dramatic separation demonstrates that our cross-model probability comparison produces more confident and well-separated membership scores than single-model or perturbation-based approaches, making it particularly valuable for auditing scenarios where false positives must be minimized.

IMDB dataset: On the IMDB dataset, the results present a notable departure from previous patterns. Ratio emerges as the top-performing method on both LLaMA-3.2-1B (Figure 2c) and Qwen-3-0.6B (Figure 2d), achieving AUCs of 95.9% and 97.4%, while HT-MIA attains 92.3% and 94.7%, the only case where our method does not achieve the highest AUC. Multiple baselines also perform substantially better on IMDB, with SPV-MIA, Zlib, and Loss all exceeding 89%. The convergence of methods at high performance levels (>88%) suggests that IMDB’s short, sentiment-driven reviews produce strong membership signals that diminish observable differences among competing approaches.

Despite not achieving the highest overall AUC, HT-MIA retains advantages in specific regions. At very low FPR (< 0.001), our method consistently outperforms all baselines except Ratio, achieving approximately 2–3× the TPR of the third-best method on LLaMA-3.2-1B and higher gains on Qwen-3-0.6B. Notably, the gap between HT-MIA and Ratio narrows substantially at $FPR < 0.0001$, with their curves nearly converging. This suggests that while Ratio’s simple likelihood ratio captures IMDB’s strong overall signal, our method provides comparable precision at the highest confidence levels and consistently outperforms all other baselines.

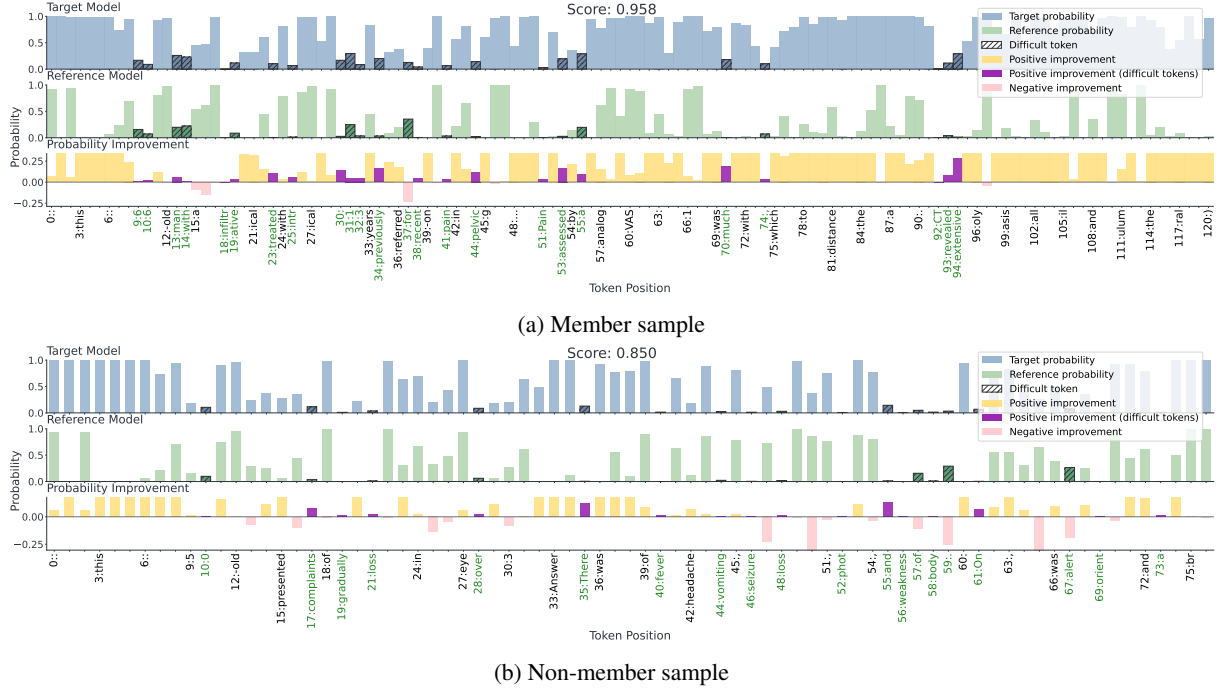


Figure 3: Token-level probability improvement across target and reference model (Clinicalnotes).

5 Ablation Studies

5.1 Effectiveness of HT-MIA

In this section, we investigate two key questions: (1) why it is necessary to measure performance improvements at low-confidence (hard) tokens rather than aggregating over entire inputs, and (2) why traditional membership inference methods fail.

Figure 3 shows a member and non-member sample from Clinicalnotes with probabilities from both target and reference models obtained from Qwen-3-0.6B. Both samples show probability improvements from reference to target model, even for non-members (Figures 3a and 3b). However, the magnitude differs: member improvements exceed 0.2, while non-member improvements barely exceed 0.1. More critically, the most difficult tokens (shown in green) reveal a pronounced distinction: about 91% improve in member samples versus only 70% in non-members. This fine-grained signal is diluted when aggregating over entire sequences, explaining why traditional methods like Loss-based or Zlib MIA fail. By focusing on the low-confidence (hard-to-predict) tokens, HT-MIA captures a much stronger membership signal. We provide further analysis in Appendix E, F, and G

5.2 Defense Against HT-MIA

To defend against HT-MIA, we incorporate DP-SGD in our LLM fine-tuning setup to evaluate the

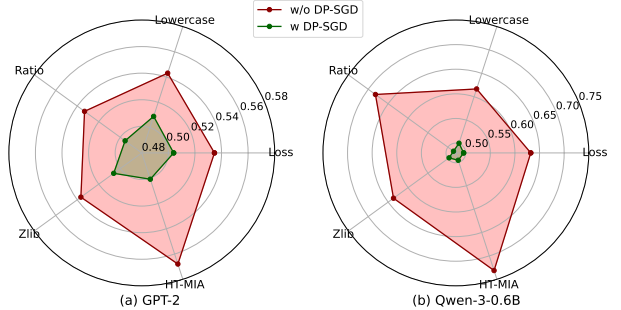


Figure 4: AUC comparison of MIA methods on GPT-2 and Qwen-3-0.6B fine-tuned with and without DP-SGD on the Asclepius dataset.

MIA defense performance as Figure 4 shows. In all cases, the AUC decreases significantly when DP-SGD is applied, demonstrating its effectiveness as a privacy-preserving mechanism. The HT-MIA AUC drops from 0.5679 to 0.5008 (a reduction of 11.8%) for GPT-2 and from 0.7312 to 0.4957 (a reduction of 32.2%) for Qwen-3-0.6B. This substantial decrease in attack effectiveness indicates that DP-SGD effectively mitigates membership inference risks and provides strong privacy protection. Similar trends are consistently observed across all baseline methods (Loss, Lowercase, Ratio, Zlib), with Qwen-3-0.6B benefiting more from DP-SGD than GPT-2. We provide the complete DP-SGD based defense results in Appendix H.

6 Related Work

Existing MIA research on LLMs can be divided into three broad categories: (1) attacks against pre-trained models, (2) attacks against fine-tuned models, and defense mechanisms.

MIA against Pre-trained Models: (Duan et al., 2024b; Meeus et al., 2025; Duan et al., 2024a) benchmark baseline MIA methods on pre-trained LLMs, finding generally poor MIA performance due to diverse pretraining corpora and n-gram overlap. (Kaneko et al., 2024) proposes SaMIA, a likelihood-independent method using sampling and n-gram overlap. (Maini et al., 2024) introduces dataset-level MIA for detecting entire training datasets. (Tao and Shokri, 2025) presents InfoMIA, a token-level information-theoretic attack that identifies memorized tokens and achieves stronger inference with fine-grained leakage localization. (Ibanez-Lissen et al., 2024) presents LU-MIA, which leverages internal hidden states rather than output likelihoods.

MIA against Fine-tuned Models: (Huang et al., 2025) proposes DF-MIA, a distribution-free attack tailored for fine-tuned LLMs. (Fu et al., 2023) introduces SPV-MIA, which builds reference datasets by self-prompting. (He et al., 2025) proposes PETAL, a label-only method using per-token semantic similarity. (Song et al., 2024) presents WEL-MIA, which assigns different weights to tokens based on their membership inference difficulty. Despite these advances, MIA research specifically targeting fine-tuned LLMs remains limited, in part due to the high computational costs associated with fine-tuning LLMs.

Defenses against MIAs: A range of defenses have been proposed to mitigate membership inference risks. Existing studies include confidence perturbation (MemGuard) (Jia et al., 2019), purification-based defenses (Yang et al., 2020), and training in membership-invariant subspaces (MIST) (Li et al., 2024). LLM-specific defenses include pruning-based approaches (Gupta et al., 2025), data transformation methods such as SOFT (Zhang et al., 2025), and soft-label training via RM Learning (Zhang et al., 2024b). Differentially Private Stochastic Gradient Descent (DP-SGD) (Abadi et al., 2016) provides formal privacy guarantees by bounding the influence of individual training samples and remains a widely adopted de-

fense against MIAs, which we adopt as an effective defense against our proposed HT-MIA.

7 Discussion

We evaluate HT-MIA against seven baseline MIA methods across four popular datasets. As shown in Section 4, HT-MIA consistently outperforms existing MIA approaches on both domain-specific and general-purpose datasets (see Tables 1, 2 and Figure 2). These results demonstrate the effectiveness of our HT-MIA method across diverse data distributions and model architectures.

Our ablation study (Section 5) reveals that while token-level probability improvements follow similar trends for members and non-members overall, they diverge sharply at low-confidence tokens (Figure 3), justifying our focus on these tokens where membership signals are most concentrated.

On the Clinicalnotes dataset, HT-MIA’s advantage over Ratio narrows at relaxed thresholds, particularly for LLaMA-3.2-1B, suggesting that simpler reference-based methods can approach sophisticated attacks when membership signals are exceptionally strong. However, HT-MIA maintains a clear advantage at strict FPR thresholds (e.g., FPR=0.01).

Dataset characteristics strongly influence MIA effectiveness. On Wikipedia, HT-MIA achieves substantial improvements (4.7-7.3% AUC), with longer, diverse articles favoring adaptive token-level analysis. In contrast, MIA performance on IMDB is slightly lower (-2.7 to -3.6%), likely due to IMDB’s short, formulaic reviews, where uniform likelihood shifts favor simpler ratio-based MIAs. Nevertheless, HT-MIA maintains enhanced MIA performance at strict FPR thresholds across all datasets, demonstrating its high value for high-precision membership inference.

8 Conclusion

We make three original contributions in this paper. *First*, we propose HT-MIA, a novel token-level membership inference attack that focuses on low-confidence (hard) tokens to capture strong membership signals. *Second*, we conduct extensive experiments demonstrating that our HT-MIA approach consistently outperforms seven representative MIA baselines across four public datasets. *Third*, through ablation studies, we explain why traditional MIA techniques underperform on fine-tuned LLMs and investigate effective defense

strategies against MIAs. Overall, this study highlights critical MIA vulnerabilities in LLMs and demonstrates the importance of fine-grained, token-level analysis for effective membership inference and privacy protection.

9 Acknowledgments

The authors acknowledge the National Science Foundation (NSF) grants IIS-2331908 and OAC-2530965, National Artificial Intelligence Research Resource (NAIRR) Pilot (NAIRR240244 and NAIRR250261), CAHSI-Google Institutional Research Program (IRP), OpenAI, and Amazon Web Services for partially contributing to this research. Any opinions, findings, and conclusions or recommendations expressed in this material are those of the author(s) and do not necessarily reflect the views of funding agencies and companies mentioned above.

References

Martin Abadi, Andy Chu, Ian Goodfellow, H Brendan McMahan, Ilya Mironov, Kunal Talwar, and Li Zhang. 2016. Deep learning with differential privacy. In *Proceedings of the 2016 ACM SIGSAC conference on computer and communications security*, pages 308–318.

Josh Achiam, Steven Adler, Sandhini Agarwal, Lama Ahmad, Ilge Akkaya, Florencia Leoni Aleman, Diogo Almeida, Janko Altenschmidt, Sam Altman, Shyamal Anadkat, and 1 others. 2023. Gpt-4 technical report. *arXiv preprint arXiv:2303.08774*.

DM Anisuzzaman, Jeffrey G Malins, Paul A Friedman, and Zachi I Attia. 2025. Fine-tuning large language models for specialized use cases. *Mayo Clinic Proceedings: Digital Health*, 3(1):100184.

Gregor Bachmann and Vaishnav Nagarajan. 2024. The pitfalls of next-token prediction. *arXiv preprint arXiv:2403.06963*.

Iz Beltagy, Kyle Lo, and Arman Cohan. 2019. Scibert: A pretrained language model for scientific text. *arXiv preprint arXiv:1903.10676*.

A. G. Bonnet and 1 others. 2023. Augmented clinical notes. HuggingFace Dataset: AGBonnet/augmented-clinical-notes.

Businessinsider. 2025. [Businessinsider](#). Accessed: September 19, 2025.

Nicholas Carlini, Steve Chien, Milad Nasr, Shuang Song, Andreas Terzis, and Florian Tramer. 2022. Membership inference attacks from first principles. In *2022 IEEE symposium on security and privacy (SP)*, pages 1897–1914. IEEE.

Nicholas Carlini, Florian Tramer, Eric Wallace, Matthew Jagielski, Ariel Herbert-Voss, Katherine Lee, Adam Roberts, Tom Brown, Dawn Song, Ulfar Erlingsson, and 1 others. 2021. Extracting training data from large language models. In *30th USENIX security symposium (USENIX Security 21)*, pages 2633–2650.

George Casella and Roger Berger. 2024. *Statistical inference*. Chapman and Hall/CRC.

Ilias Chalkidis, Manos Fergadiotis, Prodromos Malakasiotis, Nikolaos Aletras, and Ion Androutsopoulos. 2020. Legal-bert: The muppets straight out of law school. *arXiv preprint arXiv:2010.02559*.

Hongyan Chang, Ali Shahin Shamsabadi, Kleomenis Katevas, Hamed Haddadi, and Reza Shokri. 2024. Context-aware membership inference attacks against pre-trained large language models. *arXiv preprint arXiv:2409.13745*.

M Duan, A Suri, N Mireshghallah, S Min, W Shi, L Zettlemoyer, Y Tsvetkov, Y Choi, D Evans, and H Hajishirzi. 2024a. Do membership inference attacks work on large language models? *arXiv preprint arXiv:2402.07841*.

Michael Duan, Anshuman Suri, Niloofar Mireshghallah, Sewon Min, Weijia Shi, Luke Zettlemoyer, Yulia Tsvetkov, Yejin Choi, David Evans, and Hannaneh Hajishirzi. 2024b. Do membership inference attacks work on large language models? *arXiv preprint arXiv:2402.07841*.

Abhimanyu Dubey, Abhinav Jauhri, Abhinav Pandey, Abhishek Kadian, Ahmad Al-Dahle, Aiesha Letman, Akhil Mathur, Alan Schelten, Amy Yang, Angela Fan, and 1 others. 2024. The llama 3 herd of models. *arXiv e-prints*, pages arXiv–2407.

Wenjie Fu, Huandong Wang, Chen Gao, Guanghua Liu, Yong Li, and Tao Jiang. 2023. Practical membership inference attacks against fine-tuned large language models via self-prompt calibration. *arXiv preprint arXiv:2311.06062*.

fuzzy labs. 2025. [fuzzylabs](#). Accessed: October 27, 2025.

Galileo. 2025. [galileo](#). Accessed: October 27, 2025.

Mansi Gupta, Nikhar Waghela, Sarthak Gupta, Shourya Goel, and Sanjiv Shanmugavelu. 2025. Pruning as a defense: Reducing memorization in large language models. *arXiv preprint arXiv:2502.15796*.

Yu He, Boheng Li, Liu Liu, Zhongjie Ba, Wei Dong, Yiming Li, Zhan Qin, Kui Ren, and Chun Chen. 2025. Towards label-only membership inference attack against pre-trained large language models. In *USENIX Security*.

Yu He, Boheng Li, Yao Wang, Mengda Yang, Juan Wang, Hongxin Hu, and Xingyu Zhao. 2024. Is difficulty calibration all we need? towards more practical

membership inference attacks. In *Proceedings of the 2024 on ACM SIGSAC Conference on Computer and Communications Security*, pages 1226–1240.

Dan Hendrycks, Collin Burns, Steven Basart, Andy Zou, Mantas Mazeika, Dawn Song, and Jacob Steinhardt. 2020. Measuring massive multitask language understanding. *arXiv preprint arXiv:2009.03300*.

Wassily Hoeffding. 1963. Probability inequalities for sums of bounded random variables. *Journal of the American statistical association*, 58(301):13–30.

Md Millat Hosen. 2025. A lora-based approach to fine-tuning llms for educational guidance in resource-constrained settings. *arXiv preprint arXiv:2504.15610*.

Hongsheng Hu, Zoran Salcic, Lichao Sun, Gillian Dobbie, Philip S Yu, and Xuyun Zhang. 2022. Membership inference attacks on machine learning: A survey. *ACM Computing Surveys (CSUR)*, 54(11s):1–37.

Zhiheng Huang, Yannan Liu, Daojing He, and Yu Li. 2025. Df-mia: a distribution-free membership inference attack on fine-tuned large language models. In *Proceedings of the Thirty-Ninth AAAI Conference on Artificial Intelligence and Thirty-Seventh Conference on Innovative Applications of Artificial Intelligence and Fifteenth Symposium on Educational Advances in Artificial Intelligence, AAAI’25/IAAI’25/EAAI’25*. AAAI Press.

Luis Ibanez-Lissen, Lorena Gonzalez-Manzano, Jose Maria de Fuentes, Nicolas Anciaux, and Joaquin Garcia-Alfaro. 2024. Lumia: Linear probing for unimodal and multimodal membership inference attacks leveraging internal llm states. *arXiv preprint arXiv:2411.19876*.

Cheonsu Jeong. 2024. Fine-tuning and utilization methods of domain-specific llms. *arXiv preprint arXiv:2401.02981*.

Jinyuan Jia, Ahmed Salem, Michael Backes, Yang Zhang, and Neil Zhenqiang Gong. 2019. Memguard: Defending against black-box membership inference attacks via adversarial examples. In *Proceedings of the 2019 ACM SIGSAC conference on computer and communications security*, pages 259–274.

Hongpeng Jin, Wenqi Wei, Xuyu Wang, Wenbin Zhang, and Yanzhao Wu. 2023. Rethinking learning rate tuning in the era of large language models. In *2023 IEEE 5th International Conference on Cognitive Machine Intelligence (CogMI)*, pages 112–121. IEEE.

Jiandong Jin, Bowen Tang, Mingxuan Ma, Xiao Liu, Yunfei Wang, Qingnan Lai, Jia Yang, and Changling Zhou. 2024. Crimson: Empowering strategic reasoning in cybersecurity through large language models. In *2024 5th International Conference on Computer, Big Data and Artificial Intelligence (ICCBBD+ AI)*, pages 18–24. IEEE.

Qiao Jin, Bhuwan Dhingra, Zhengping Liu, William Cohen, and Xinghua Lu. 2019. Pubmedqa: A dataset for biomedical research question answering. In *Proceedings of the 2019 conference on empirical methods in natural language processing and the 9th international joint conference on natural language processing (EMNLP-IJCNLP)*, pages 2567–2577.

Masahiro Kaneko, Youmi Ma, Yuki Wata, and Naoaki Okazaki. 2024. Sampling-based pseudo-likelihood for membership inference attacks. *arXiv preprint arXiv:2404.11262*.

S. Kweon and 1 others. 2023. Asclepius synthetic clinical notes. HuggingFace Dataset: starmpcc/Asclepius-Synthetic-Clinical-Notes.

Jiacheng Li, Ninghui Li, and Bruno Ribeiro. 2024. {MIST}: Defending against membership inference attacks through {Membership-Invariant} subspace training. In *33rd USENIX Security Symposium (USENIX Security 24)*, pages 2387–2404.

Renqian Luo, Lai Sun, Yingce Xia, Tao Qin, Sheng Zhang, Hoifung Poon, and Tie-Yan Liu. 2022. Biogpt: generative pre-trained transformer for biomedical text generation and mining. *Briefings in bioinformatics*, 23(6):bbac409.

Andrew L. Maas, Raymond E. Daly, Peter T. Pham, Dan Huang, Andrew Y. Ng, and Christopher Potts. 2011. Learning word vectors for sentiment analysis. In *Proceedings of the 49th Annual Meeting of the Association for Computational Linguistics: Human Language Technologies*, page 142–150.

Pratyush Maini, Hengrui Jia, Nicolas Papernot, and Adam Dziedzic. 2024. Llm dataset inference: Did you train on my dataset? *Advances in Neural Information Processing Systems*, 37:124069–124092.

Sadhika Malladi, Tianyu Gao, Eshaan Nichani, Alex Damian, Jason D Lee, Danqi Chen, and Sanjeev Arora. 2023. Fine-tuning language models with just forward passes. *Advances in Neural Information Processing Systems*, 36:53038–53075.

Matthieu Meeus, Shubham Jain, Marek Rei, and Yves-Alexandre de Montjoye. 2024. Did the neurons read your book? document-level membership inference for large language models. In *33rd USENIX Security Symposium (USENIX Security 24)*, pages 2369–2385.

Matthieu Meeus, Igor Shilov, Shubham Jain, Manuel Faysse, Marek Rei, and Yves-Alexandre de Montjoye. 2025. Sok: Membership inference attacks on llms are rushing nowhere (and how to fix it). In *2025 IEEE Conference on Secure and Trustworthy Machine Learning (SaTML)*, pages 385–401. IEEE.

Fatemehsadat Mireshghallah, Kartik Goyal, Archit Uniyal, Taylor Berg-Kirkpatrick, and Reza Shokri. 2022. Quantifying privacy risks of masked language models using membership inference attacks. *arXiv preprint arXiv:2203.03929*.

Joel Niklaus, Lucia Zheng, Arya D McCarthy, Christopher Hahn, Brian M Rosen, Peter Henderson, Daniel E Ho, Garrett Honke, Percy Liang, and Christopher Manning. 2024. Flawn-t5: An empirical examination of effective instruction-tuning data mixtures for legal reasoning. *arXiv preprint arXiv:2404.02127*.

Pedro Henrique Paiola, Gabriel Lino Garcia, Joao Renato Ribeiro Manesco, Mateus Roder, Douglas Rodrigues, and Joao Paulo Papa. 2024. Adapting llms for the medical domain in portuguese: A study on fine-tuning and model evaluation. *arXiv preprint arXiv:2410.00163*.

Ankit Pal, Logesh Kumar Umapathi, and Malaikanan Sankarasubbu. 2022. Medmcqa: A large-scale multi-subject multi-choice dataset for medical domain question answering. In *Conference on health, inference, and learning*, pages 248–260. PMLR.

Alec Radford, Jeffrey Wu, Rewon Child, David Luan, Dario Amodei, Ilya Sutskever, and 1 others. 2019. Language models are unsupervised multitask learners. *OpenAI blog*, 1(8):9.

Emily Ross, Yuval Kansal, Jake Renzella, Alexandra Vassar, and Andrew Taylor. 2025. Supervised fine-tuning llms to behave as pedagogical agents in programming education. *arXiv preprint arXiv:2502.20527*.

Ivan Montoya Sanchez, Shaswata Mitra, Aritran Piplai, and Sudip Mittal. 2025. Semantic-aware contrastive fine-tuning: Boosting multimodal malware classification with discriminative embeddings. *arXiv preprint arXiv:2504.21028*.

Victor Sanh, Lysandre Debut, Julien Chaumond, and Thomas Wolf. 2019. Distilbert, a distilled version of bert: smaller, faster, cheaper and lighter. *arXiv preprint arXiv:1910.01108*.

Alexander Scarlatos, Naiming Liu, Jaewook Lee, Richard Baraniuk, and Andrew Lan. 2025. Training llm-based tutors to improve student learning outcomes in dialogues. In *International Conference on Artificial Intelligence in Education*, pages 251–266. Springer.

Reza Shokri, Marco Stronati, Congzheng Song, and Vitaly Shmatikov. 2017. Membership inference attacks against machine learning models. In *2017 IEEE symposium on security and privacy (SP)*, pages 3–18. IEEE.

Karan Singhal, Shekoofeh Azizi, Tao Tu, S Sara Mhdavi, Jason Wei, Hyung Won Chung, Nathan Scales, Ajay Tanwani, Heather Cole-Lewis, Stephen Pfohl, and 1 others. 2023. Large language models encode clinical knowledge. *Nature*, 620(7972):172–180.

Changtian Song, Dongdong Zhao, and Jianwen Xiang. 2024. Not all tokens are equal: Membership inference attacks against fine-tuned language models. In *2024 Annual Computer Security Applications Conference (ACSAC)*, pages 31–45. IEEE.

Jiashu Tao and Reza Shokri. 2025. (token-level) informia: Stronger membership inference and memorization assessment for llms. *arXiv preprint arXiv:2510.05582*.

Ross Taylor, Marcin Kardas, Guillem Cucurull, Thomas Scialom, Anthony Hartshorn, Elvis Saravia, Andrew Poulton, Viktor Kerkez, and Robert Stojnic. 2022. Galactica: A large language model for science. *arXiv preprint arXiv:2211.09085*.

Amit Tewari. 2024. Legalpro-bert: Classification of legal provisions by fine-tuning bert large language model. *arXiv preprint arXiv:2404.10097*.

Guangyu Wang, Guoxing Yang, Zongxin Du, Longjun Fan, and Xiaohu Li. 2023. Clinicalgpt: large language models finetuned with diverse medical data and comprehensive evaluation. *arXiv preprint arXiv:2306.09968*.

Wikipedia. 2022. Wikipedia dataset (english, march 2022 dump). Hugging Face: <https://huggingface.co/datasets/wikipedia>. Configuration: 20220301.en, Accessed: January 2025.

Chaoyi Wu, Xiaoman Zhang, Ya Zhang, Yanfeng Wang, and Weidi Xie. 2023. Pmc-llama: Further fine-tuning llama on medical papers. *arXiv preprint arXiv:2304.14454*, 2(5):6.

An Yang, Anfeng Li, Baosong Yang, Beichen Zhang, Binyuan Hui, Bo Zheng, Bowen Yu, Chang Gao, Chengan Huang, Chenxu Lv, and 1 others. 2025. Qwen3 technical report. *arXiv preprint arXiv:2505.09388*.

Ziqi Yang, Bin Shao, Bohan Xuan, Ee-Chien Chang, and Fan Zhang. 2020. Defending model inversion and membership inference attacks via prediction purification. *arXiv preprint arXiv:2005.03915*.

Wentao Ye, Jiaqi Hu, Liyao Li, Haobo Wang, Gang Chen, and Junbo Zhao. 2024. Data contamination calibration for black-box llms. *arXiv preprint arXiv:2405.11930*.

Samuel Yeom, Irene Giacomelli, Matt Fredrikson, and Somesh Jha. 2018. Privacy risk in machine learning: Analyzing the connection to overfitting. In *2018 IEEE 31st computer security foundations symposium (CSF)*, pages 268–282. IEEE.

Jingyang Zhang, Jingwei Sun, Eric Yeats, Yang Ouyang, Martin Kuo, Jianyi Zhang, Hao Frank Yang, and Hai Li. 2024a. Min-k%++: Improved baseline for detecting pre-training data from large language models. *arXiv preprint arXiv:2404.02936*.

Kaiyuan Zhang, Siyuan Cheng, Hanxi Guo, Yuetian Chen, Zian Su, Shengwei An, Yuntao Du, Charles Fleming, Ashish Kundu, Xiangyu Zhang, and 1 others. 2025. Soft: Selective data obfuscation for protecting llm fine-tuning against membership inference attacks. *arXiv preprint arXiv:2506.10424*.

Liwei Zhang, Linghui Li, Xiaoyong Li, Binsi Cai, Yali Gao, Ruobin Dou, and Luying Chen. 2023. Efficient membership inference attacks against federated learning via bias differences. In *Proceedings of the 26th international symposium on research in attacks, intrusions and defenses*, pages 222–235.

Zheng Zhang, Jianfeng Ma, Xindi Ma, Ruikang Yang, Xiangyu Wang, and Junying Zhang. 2024b. Defending against membership inference attacks: Rm learning is all you need. *Information Sciences*, 670:120636.

Ziqi Zhang, Chao Yan, and Bradley A Malin. 2022. Membership inference attacks against synthetic health data. *Journal of biomedical informatics*, 125:103977.

Da Zhong, Xiuling Wang, Zhichao Xu, Jun Xu, and Wendy Hui Wang. 2024. Interaction-level membership inference attack against recommender systems with long-tailed distribution. In *Proceedings of the 33rd ACM International Conference on Information and Knowledge Management*, pages 3433–3442.

In the appendix, we provide additional material and technical details.

A Theoretical Analysis

We present formal analysis justifying our design choices and establishing the statistical properties of the HT-MIA score. Our method makes three key design decisions: (1) using binary indicators $\mathbf{1}\{\Delta_i > 0\}$ rather than raw probability differences, which provides robustness to outliers and yields interpretable scores in $[0, 1]$; (2) normalizing by $1/K$ to ensure comparability across texts of different lengths; and (3) adaptively selecting $K = \min(\max_k, \max(\min_k, \lfloor \alpha L \rfloor))$ to balance signal strength, computational efficiency, and stability across short and long sequences. We now formalize why these choices are optimal.

Lemma 1 (Informative-token focus). Let $\mu_i := \mathbb{E}[\Delta_i \mid x \in D_{\text{mem}}] - \mathbb{E}[\Delta_i \mid x \in D_{\text{non}}]$ be the member–non-member mean gap at token i . Assume that $|\mu_i|$ is non-increasing in $p_{\mathcal{F},i}$, so that harder tokens under \mathcal{F} carry at least as much membership signal. Then, for any subset size K , the set I_{\min} of the K smallest $p_{\mathcal{F},i}$ maximizes $\sum_{i \in I} |\mu_i|$ over all $I \subseteq \{1, \dots, L\}$ with $|I| = K$.

Proof. Order tokens so that $p_{\mathcal{F},(1)} \leq \dots \leq p_{\mathcal{F},(L)}$ implies $|\mu_{(1)}| \geq \dots \geq |\mu_{(L)}|$. Maximizing $\sum_{i \in I} |\mu_i|$ over $|I| = K$ is achieved by selecting the K largest $|\mu_i|$, which corresponds to I_{\min} by rearrangement inequality.

Lemma 1 formalizes why focusing on low-probability tokens (lines 10-13 of Algorithm 1) is

optimal: under the natural assumption that difficult tokens carry more membership signal than easy tokens, selecting I_{\min} maximizes total discriminative power. This assumption is well-motivated: high-probability tokens are already well-predicted by both models, leaving minimal room for \mathcal{F} to demonstrate memorization, while low-probability positions represent challenging predictions where fine-tuning effects are most pronounced.

Lemma 2 (Neyman-Pearson optimality). Let $Z_i := \mathbf{1}\{\Delta_i > 0\}$ for $i \in I_{\min}$ and define $S = \frac{1}{K} \sum_{i \in I_{\min}} Z_i$. Suppose S has densities p_{mem} and p_{non} for member and non-member texts, and that the likelihood ratio $p_{\text{mem}}(s)/p_{\text{non}}(s)$ is monotone increasing in s . Then, among all tests with a fixed false-positive rate, the threshold rule $g(x; \mathcal{F}) = \text{member} \iff S(x; \mathcal{F}, \mathcal{B}) \geq \tau$ is most powerful.

Proof. Under monotone likelihood ratio in s , the uniformly most powerful level- α test is a threshold on s by the Neyman–Pearson lemma (Casella and Berger, 2024). The MLR property holds when Z_i are i.i.d. Bernoulli with $p_{\text{mem}} > p_{\text{non}}$.

Lemma 2 establishes that thresholding the HT-MIA score (line 15 of Algorithm 1) is statistically optimal: among all decision rules maintaining a fixed false-positive rate, it achieves maximum power. This means practitioners need not search for complex decision boundaries. A simple threshold yields the optimal decision and is provably best.

Theorem 1 (Finite-sample detection guarantees). Assume $\{Z_i\}_{i \in I_{\min}}$ are independent and bounded in $[0, 1]$, with $\mathbb{E}[Z_i \mid x \in D_{\text{mem}}] = p_{\text{mem}}$ and $\mathbb{E}[Z_i \mid x \in D_{\text{non}}] = p_{\text{non}}$, where $p_{\text{mem}} > p_{\text{non}}$. For any threshold $\tau \in (0, 1)$ and any $K \geq 1$,

$$\mathbb{P}[S \leq \tau \mid x \in D_{\text{mem}}] \leq \exp(-2K(p_{\text{mem}} - \tau)^2),$$

$$\mathbb{P}[S \geq \tau \mid x \in D_{\text{non}}] \leq \exp(-2K(\tau - p_{\text{non}})^2).$$

Proof. The score $S = \frac{1}{K} \sum_{i \in I_{\min}} Z_i$ is the average of K independent variables in $[0, 1]$ with $\mathbb{E}[S \mid x \in D_{\text{mem}}] = p_{\text{mem}}$ and $\mathbb{E}[S \mid x \in D_{\text{non}}] = p_{\text{non}}$. Applying Hoeffding’s inequality (Hoeffding, 1963) with deviations $t = p_{\text{mem}} - \tau$ and $t = \tau - p_{\text{non}}$ yields the stated bounds.

Corollary 1 (Sample complexity for target power). Let $\gamma := p_{\text{mem}} - p_{\text{non}} > 0$ and choose any $\tau \in (p_{\text{non}}, p_{\text{mem}})$. If $K \geq \frac{1}{2\gamma^2} \log \frac{1}{\beta}$, then the test attains power at least $1 - \beta$ at the chosen false-positive rate.

Proof. Setting the first bound in Theorem 1 equal to β and solving for K gives $K \geq \frac{\log(1/\beta)}{2(p_{\text{mem}} - \tau)^2}$. Choos-

ing τ optimally between p_{non} and p_{mem} and using $\gamma = p_{\text{mem}} - p_{\text{non}}$ yields the stated bound.

Theorem 1 provides exponential concentration guarantees: both error types decay exponentially in K . Corollary 1 quantifies exactly how many tokens are needed for reliable detection—even moderate values like $K \approx 20\text{-}50$ suffice when the gap $\gamma = p_{\text{mem}} - p_{\text{non}}$ is reasonably sized. This explains why our adaptive K selection (lines 10-11 of Algorithm 1) is effective: by scaling K with sequence length through αL while respecting practical bounds (min_k , max_k), detection reliability automatically adapts to available signal. For longer sequences, larger K provides stronger concentration; for shorter sequences, min_k ensures adequate power.

Together, these results establish that HT-MIA is both theoretically principled and practically efficient: (1) selecting low-probability tokens is provably optimal (Lemma 1), (2) the threshold-based decision rule is most powerful among all alternatives (Lemma 2), and (3) finite-sample error bounds decay exponentially with sequence length (Theorem 1). All guarantees hold with a simple, efficient algorithm requiring only two forward passes, making the method scalable to real-world applications. While our results rely on independence assumptions, the method exhibits robustness in practice: mild token dependencies degrade performance gracefully, and the approach remains effective even when the reference model \mathcal{B} is not exactly the pre-fine-tuning checkpoint.

B Baselines

To compare HT-MIA, we evaluate against seven established MIA attack methods.

Loss. The *Loss*-based attack (Yeom et al., 2018) infers membership by using the per-sample cross-entropy loss, under the assumption that training samples generally achieve lower loss values than non-members:

$$L(x, y) = -\log p_{\theta}(y | x), \quad (8)$$

where x denotes the input text, y is the target output, and $p_{\theta}(y | x)$ represents the model’s predicted probability for y given x under parameters θ . Lower loss values suggest the model is more confident in its predictions, which is typical for training samples, making $L(x, y)$ an effective membership signal. Samples with $L(x, y)$ below a chosen threshold are classified as members.

Lowercase. The *Lowercase* attack (Carlini et al.,

2021) evaluates memorization by measuring the change in model perplexity when the input text is normalized to lowercase form:

$$\Delta\text{PPL} = \text{PPL}(x) - \text{PPL}(\text{lowercase}(x)), \quad (9)$$

where $\text{PPL}(x) = \exp(L(x))$ is the perplexity of the original text computed as the exponential of the average per-token negative log-likelihood, and $\text{lowercase}(x)$ denotes the text with all characters converted to lowercase. Memorized sequences are typically more sensitive to this perturbation, producing larger changes in perplexity ($\Delta\text{PPL} > 0$) compared to non-members, which exhibit more robust predictions.

Min-K++. The *Min-K++* (Zhang et al., 2024a) method identifies membership by focusing on the least likely $k\%$ tokens in a sequence and normalizing their probabilities:

$$\text{Min-K}^{++}(x) = \frac{1}{|k\%|} \sum_{t \in \text{min-}k\%} \frac{\log p_{\theta}(x_t | x_{<t}) - \mu}{\sigma}, \quad (10)$$

where x_t is the token at position t , $x_{<t}$ represents all preceding tokens, $p_{\theta}(x_t | x_{<t})$ is the model’s predicted probability for token x_t given its context, and $\text{min-}k\%$ denotes the set of token positions corresponding to the lowest $k\%$ of probabilities in the sequence. The term $|k\%|$ denotes the number of tokens selected. μ and σ are the mean and standard deviation of log-probabilities computed over all tokens in the sequence x . This z-score normalization accounts for per-sequence variability in token difficulty, making the score more robust across texts with different intrinsic complexity levels. Higher scores indicate membership.

PAC. The *PAC* attack (Ye et al., 2024) contrasts a polarized token–log-probability distance on the original text with the average over augmented neighbors $\mathcal{A}(x)$:

$$\text{PAC}(x) = \text{PD}(x) - \frac{1}{|\mathcal{A}(x)|} \sum_{\tilde{x} \in \mathcal{A}(x)} \text{PD}(\tilde{x}), \quad (11)$$

where $\text{PD}(x)$ denotes the *polarized distance*, defined as the difference between the mean log-probabilities of the top- k and bottom- k tokens in sequence x . The set $\mathcal{A}(x)$ contains augmented versions of x generated through paraphrasing or perturbation operations, and $|\mathcal{A}(x)|$ is the number of such augmentations. The second term represents the average polarized distance over these neighbors. The intuition is that member texts exhibit a larger gap between easy and hard tokens compared to their augmented variants, as memorization creates sharp probability contrasts that are disrupted by text modification.

Ratio. The *Ratio* attack (Carlini et al., 2021) compares the per-sample negative log-likelihood (NLL) under the target model to that under a fixed reference model:

$$\text{Ratio}(x) = -\frac{\text{NLL}_{\text{tgt}}(x)}{\text{NLL}_{\text{ref}}(x)}, \quad (12)$$

where $\text{NLL}_{\text{tgt}}(x) = -\sum_t \log p_{\theta_{\text{tgt}}}(x_t | x_{<t})$ is the negative log-likelihood under the target (fine-tuned) model with parameters θ_{tgt} , and $\text{NLL}_{\text{ref}}(x)$ is the corresponding quantity under a reference model with parameters θ_{ref} . The negative sign ensures that more negative ratios (indicating lower loss on the target model relative to the reference) correspond to higher membership likelihood. This method captures relative improvement: members should have lower NLL under the target model compared to the baseline reference.

Zlib. The *Zlib*-based attack (Carlini et al., 2021) contrasts model fit with text compressibility:

$$\text{Zlib}(x) = -\frac{L(x)}{\text{zlibEntropy}(x)}, \quad (13)$$

where $L(x) = -\frac{1}{|x|} \sum_t \log p_{\theta}(x_t | x_{<t})$ is the per-token average NLL under the model, and $\text{zlibEntropy}(x) = \frac{\text{len}(\text{zlib.compress}(x))}{\text{len}(x)}$ is the compressed size per character obtained by applying the zlib compression algorithm to the text. The intuition is that memorized texts have low model loss $L(x)$ relative to their intrinsic complexity measured by compression. A small ratio (more negative score) suggests the model fits the text better than its complexity warrants, indicating memorization. Samples with more negative $\text{Zlib}(x)$ scores are classified as members.

SPV-MIA. The *SPV-MIA* (Self-calibrated Probabilistic Variation) attack (Fu et al., 2023) measures probabilistic variation by comparing model probabilities on paraphrased versus original text:

$$\text{SPV}(x) = [\bar{p}_{\theta}(\tilde{x}) - p_{\theta}(x)] - [\bar{p}_{\hat{\theta}}(\tilde{x}) - p_{\hat{\theta}}(x)], \quad (14)$$

where $\bar{p}_{\theta}(\tilde{x}) = \frac{1}{N} \sum_{i=1}^N p_{\theta}(\tilde{x}_i)$ is the mean probability assigned by the target model with parameters θ to N paraphrased versions \tilde{x}_i generated via T5-based mask-filling, $p_{\theta}(x)$ is the probability on the original text. $\bar{p}_{\hat{\theta}}(\tilde{x})$, $p_{\hat{\theta}}(x)$ are the corresponding quantities on a self-prompt reference model with parameters $\hat{\theta}$. The reference model is fine-tuned on text generated by prompting the target model itself, enabling calibration without access to the original training data. The intuition is that memorized texts exhibit smaller probability variation across paraphrases on the target model compared

to the reference model. Because member texts resist such perturbations due to memorization, they yield higher calibrated scores. Samples with more positive $\text{SPV}(x)$ values are classified as members.

C Evaluation Metrics

To evaluate the effectiveness of HT-MIA, we report the Area Under the ROC Curve (AUC) and the True Positive Rate (TPR) at fixed False Positive Rate (FPR) (Carlini et al., 2022). The outcomes of the attack classifier are summarized by the standard quantities of true positives (TP), false positives (FP), true negatives (TN), and false negatives (FN).

True Positive Rate (TPR). The TPR measures the fraction of member samples correctly classified as members:

$$\text{TPR} = \frac{TP}{TP + FN}. \quad (15)$$

False Positive Rate (FPR). The FPR measures the fraction of non-member samples incorrectly classified as members:

$$\text{FPR} = \frac{FP}{FP + TN}. \quad (16)$$

In our evaluation, we report $\text{TPR}@FPR=0.1$ and $\text{TPR}@FPR=0.01$, which quantify the attack’s detection power under strict false-positive constraints.

ROC Curve and Area Under the Curve (AUC). The ROC curve plots TPR against FPR across varying decision thresholds of the attack classifier. The area under the ROC curve (AUC) provides a threshold-independent measure of discrimination power:

$$\text{AUC} = \int_0^1 \text{TPR}(\text{FPR}) d(\text{FPR}). \quad (17)$$

AUC values range from 0.5 (random guessing) to 1.0 (perfect classification), with higher values indicating better MIA performance.

D Analysis of Token-Level Probability Distribution on IMDB

Figure 5 shows similar patterns on IMDB. However, this also explains why HT-MIA fails to surpass Ratio on IMDB. IMDB non-member tokens include generic terms like index 13: man, 18: show, 37: school, 50: cartoon, which are likely in pretraining data. In contrast, Clinicalnotes non-member tokens include domain-specific terms like index 44: vomiting, 46: seizure, 56: weakness, 58: body, 67: alert (Figure 3). Datasets with domain-specific tokens highlight probability improvements more distinctly, giving HT-MIA a clearer advantage over simpler methods like Ratio.

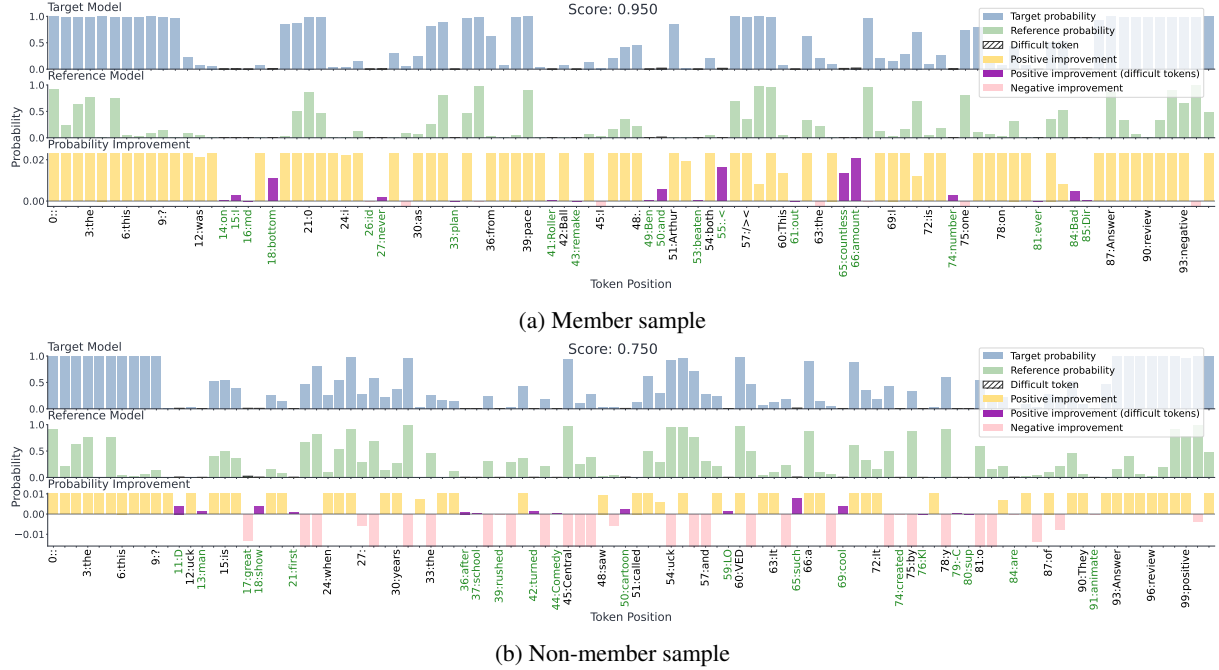


Figure 5: Token-level probability improvement across target and reference model (IMDB).

E Effect of Threshold on HT-MIA Performance

In Table 3 and 4 we provide a direct analysis of varying threshold by explicitly changing τ . As observed, very low thresholds ($\tau \in [0.1, 0.3]$) result in poor AUC performance. As the threshold increases, the AUC improves, reaching its peak at $\tau = 0.6$ with an AUC of 80.77%. Beyond this point, performance begins to degrade. At $\tau = 0.7$, the AUC drops to 76.35%, and at $\tau = 0.9$, it decreases further to 53.77%.

A similar trend is observed on the Wikipedia dataset. Very low thresholds ($\tau \in [0.1, 0.2]$) again yield poor performance, with the AUC improving steadily as the threshold increases. The optimal performance is achieved at $\tau = 0.5$ with an AUC of 83.81%, remaining nearly stable at $\tau = 0.6$ (83.59%). Performance then degrades at higher thresholds, dropping to 74.68% at $\tau = 0.7$ and 51.58% at $\tau = 0.9$.

Threshold	0.1	0.2	0.3	0.4	0.5	0.6	0.7	0.8	0.9
AUC	0.5015	0.5143	0.5615	0.6606	0.7676	0.8077	0.7635	0.6425	0.5377

Table 3: AUC results across different thresholds for HT-MIA on Qwen-3-0.6B with Clinicalnotes dataset.

Threshold	0.1	0.2	0.3	0.4	0.5	0.6	0.7	0.8	0.9
AUC	0.5002	0.5107	0.5834	0.7286	0.8381	0.8359	0.7468	0.6085	0.5158

Table 4: AUC results across different thresholds for HT-MIA on Qwen-3-0.6B with Wikipedia dataset.

F Effect of Model Choice on Token Selection

In our main experiment, the HT-MIA algorithm uses the target model’s token-level probability distribution to identify the most problematic tokens. In Table 5 we experiment by switching the algorithm to use the reference model for token selection.

Token Selection Strategy	Qwen-3-0.6B	LLaMA-3.2-1B
Target Model	0.8843	0.8659
Reference Model	0.8648	0.8474

(a) AUC		
Token Selection Strategy	Qwen-3-0.6B	LLaMA-3.2-1B
Target Model	0.6861	0.7057
Reference Model	0.6999	0.6901

(b) TPR@FPR=0.1		
Token Selection Strategy	Qwen-3-0.6B	LLaMA-3.2-1B
Target Model	0.3839	0.4253
Reference Model	0.2986	0.3545

(c) TPR@FPR=0.01		
Token Selection Strategy	Qwen-3-0.6B	LLaMA-3.2-1B
Target Model	0.3839	0.4253
Reference Model	0.2986	0.3545

Table 5: Effect of the target model vs. the reference model on token selection on Target models fine-tuned on Clinicalnotes dataset.

Both in terms of AUC and TPR@FPR=0.01, the performance shows a slight decrease (AUC drops by about 2.1% for LLaMA-3.2-1B). However, for the more relaxed case of TPR@FPR=0.1, Qwen exhibits a small improvement (about 2.0%), whereas LLaMA-3 still decreases slightly (around 2.2%).

G Effect of Reference Model on HT-MIA Performance

For our primary results, we utilize the same base pretrained version of the target model as the reference, though in practice an attacker is unlikely to have access to a reference model identical to the target’s base. To mimic this, we experiment with models that share a similar tokenizer but belong to different variants within the same model family in Tables 6 and 7.

Specifically, for the target Qwen-3-0.6B, we compare against a reference model Qwen-2.5-0.5B, and for the target GPT-2, we use DistilGPT-2 as the reference.

As expected, the results show a moderate drop in performance. For Qwen-3-0.6B, the AUC decreases from 88.43% to 87.20%, corresponding to a 1.4% relative drop. For GPT-2, the AUC decreases from 69.77% to 66.74%, corresponding to a 4.3% relative drop.

Reference Model	AUC	TPR@FPR=0.1	TPR@FPR=0.01
Qwen-3-0.6B	0.8843	0.6861	0.3839
Qwen-2.5-0.5B	0.8720	0.6818	0.2765

Table 6: Effect of Reference model on HT-MIA performance on Target model Qwen-3-0.6B fine-tuned on Clinicalnotes dataset.

Reference Model	AUC	TPR@FPR=0.1	TPR@FPR=0.01
GPT-2	0.6977	0.3222	0.0522
DistilGPT-2	0.6674	0.2603	0.0540

Table 7: Effect of Reference model on HT-MIA performance on Target model GPT-2 fine-tuned on Clinicalnotes dataset.

H Effect on Post Fine-tuning Performance due to DP-SGD

To evaluate the privacy-utility tradeoff, we assess model performance on four downstream medical QA tasks (MedMCQA, Clinical Knowledge, College Biology, and PubMedQA (Pal et al., 2022; Hendrycks et al., 2020; Jin et al., 2019)). As shown

Task	Qwen-3-0.6B		GPT-2	
	FT	DP-SGD	FT	DP-SGD
MedMCQA	0.2890	0.2893	0.2921	0.2649
Clinical Knowledge	0.2679	0.2151	0.2642	0.2453
College Biology	0.2569	0.2569	0.2929	0.2361
PubMedQA	0.5580	0.4620	0.4800	0.3240

Table 8: Three-shot downstream task accuracy comparison between standard fine-tuning (FT) and DP-SGD fine-tuning on the Asclepius dataset for Qwen-3-0.6B and GPT-2.

in Table 8, the application of DP-SGD during fine-tuning reduces downstream task performance for both models, demonstrating the inherent privacy-utility tradeoff. For GPT-2, DP-SGD results in accuracy drops across most tasks: MedMCQA decreases by 9.3% (from 0.2921 to 0.2649), Clinical Knowledge by 7.2% (from 0.2642 to 0.2453), College Biology by 19.4% (from 0.2929 to 0.2361), and PubMedQA by 32.5% (from 0.4800 to 0.3240). For Qwen-3-0.6B, DP-SGD has minimal impact on MedMCQA and College Biology, but significantly degrades performance on Clinical Knowledge (19.7% drop) and PubMedQA (17.2% drop). These results confirm that while DP-SGD provides strong privacy guarantees as demonstrated in Figure 4, it comes at the cost of reduced model utility on downstream medical QA tasks.